Analysis of interface kinetics: solutions of the Gibbs-Thomson-type equation and of the kinetic rate theory

A Salhoumi[1,2] and P K Galenko[3,4]

[1] University of Hassan II Casablanca, Faculty of Sciences Ben M'Sik, Department of Physics, Laboratory of Condensed Matter Physics (LPMC), BP 7955 Casablanca, Morocco
[2] University of Hassan II Casablanca, Faculté des Sciences Juridiques, Economiques et Sociales Ain Sebaa, Département des Statistiques et Mathématiques Appliquées à l'Economie et à la Gestion (SMAEG), Laboratoire de la Modélisation Appliquée à l'Economie et à la Gestion (MAEG), BP 2634 Casablanca, Morocco
[3] Friedrich-Schiller-Universität Jena, Physikalisch-Astronomische Fakultät, D-07743 Jena, Germany
[4] Ural Federal University, Laboratory of Multi-Scale Mathematical Modeling, 620002 Ekaterinburg, Russia

E-mail: `peter.galenko@uni-jena.de` · `ahmedsalhoumi@gmail.com`

Abstract. Rapidly moving solid-liquid interface is treated analytically and numerically. Derivation and qualitative analysis of interface propagation kinetics is presented. Quantitative predictions of solutions, which follow from the Kinetic Rate Theory and the solution of Gibbs-Thomson-type equation, are compared with Molecular Dynamics simulation data (MD-data) on crystallization and melting of fcc-lattice of nickel. It is shown in the approximation of a linear behavior of the interface velocity versus undercooling that the Gibbs-Thomson-type equation and kinetic rate theory describe MD-data well enough, in the range of small growth velocity and within the range of relatively small undercooling, with a relative error for the obtained values of kinetic coefficient of the order 1.1%. Within the small-and long range of undercooling, in nonlinear behavior of the interface velocity versus undercooling, the kinetic rate theory disagrees sharply with MD-data, qualitatively and quantitatively, unlike to the Gibbs-Thomson-type equation which is in a good agreement with MD-data within the whole range of undercooling and crystal growth velocity.

1. Introduction

Methods of atomistic simulation represent now the robust quantitative techniques, which serve to obtain equilibrium and kinetic properties of phase interfaces. In equilibrium, these properties concern the surface energy and have physical relevance for the atomistic thickness of interfaces. In dynamics, these properties are connected to the interfacial self- and inter-diffusion as well as the mobility of interfaces. The latter property plays a crucial role in the description of both the interface propagation and pattern formation [1]. Indeed, special attention in atomistic simulations is paid to melting/crystallization kinetics and diffusion dynamics [2, 3]. More specifically, using MD-data of simulation [4, 5], as well as verification of various kinetic models and tests of phase field models have been provided [1, 6, 7].

In the present work, we use MD-data as a benchmark to verify outcomes from two theoretical approaches: the Kinetic Rate Theory (KRT) and Phase Field Model (PFM). We shall check both the qualitative behavior and the quantitative consistency of the kinetic equation for interface motion and acceleration dependent Gibbs-Thomson equation with respect to MD-data for solidification and melting of nickel crystal growing in the $< 100 >$–direction.

2. Kinetic rate theory

The Kinetic Rate Theory (or "the theory of rate kinetics") describes the interface motion due to the driving force which provides the overcome of an energetic barrier between the phases that have different energies [8]. In this section, we briefly describe the Kinetic Rate Theory due to Chernov [9]. This theory is applied to the growing crystal from an undercooled melt. When a particle (atom, molecule, or ion), moves from the crystal into the medium under the equilibrium conditions, it must change its energy by

$$\varepsilon_M - \varepsilon_S = T_m \left(s_M - s_S \right) \equiv \Delta H. \tag{1}$$

where ε_S and ε_M are the average energies of the particles, which occupy the equilibrium positions in the crystal and the medium, T_m is the melting temperature, s_S and s_M are the entropy in solid and in the medium, respectively, and ΔH is the enthalpy of the melting.

At the crystal-liquid interface, the particle must generally overcome a potential barrier E ("the activation energy" E) which depends on the configuration of the activated complex in the liquid. The real role is played by the value of E which is minimal with respect to the various configurations of the activation complex. These interfacial configurations depend on the structures of both the liquid and the solid phases, and the probability that the complex most suitable for the transition will appear is determined by the easiness with which the short-range order in the liquid changes to that in the solid. The atomic configurations also change in a viscous flow of the liquid. Therefore for the crystal-melt interface, E was expected to have the values of the order of the activation energy for a viscous flow.

The numbers j_+ of atoms that go from the melt over the crystal per unit time at a single kink (interface), and the opposite flow j_- from crystal to the melt can be written as

$$j_+ \;=\; \widetilde{\nu} \exp \left(-\frac{\Delta s}{k} \right) \exp \left(-\frac{E}{kT} \right), \tag{2}$$

$$j_- \;=\; \widetilde{\nu} \exp \left(-\frac{\Delta s}{k} \right) \exp \left(-\frac{E + \Delta H}{kT} \right). \tag{3}$$

where $\widetilde{\nu}$ is the frequency of thermal vibrations of an atom in the crystal and the liquid, Δs is the entropy of the melting, T is the absolute temperature, k is Boltzmann's constant, and $\exp \left(-\Delta s / k \right)$ is the probability of finding an atom of the liquid in the immediate vicinity of the kink in the most advantageous activation complex corresponding to barrier E.

If the average distance between the kinks is λ_0, the probability of finding a kink on the surface is equal to $(a/\lambda_0)^2$ with a the crystal lattice parameter. Then, the velocity of the phase boundary is given by

$$V = \left(\frac{a}{\lambda_0} \right)^2 a \left(j_+ - j_- \right)$$

$$= \left(\frac{a}{\lambda_0} \right)^2 a \widetilde{\nu} \exp \left(-\frac{\Delta s}{k} \right) \exp \left(-\frac{E}{kT} \right) \left\{ 1 - \exp \left[-\frac{\Delta H}{k} \left(\frac{1}{T} - \frac{1}{T_m} \right) \right] \right\}. \tag{4}$$

which is reduced in the condition $\Delta s \Delta T / kT \ll 1$, i.e., the condition of low undercooling at growth front such as

$$V \simeq \beta \left(T \right) \Delta T . \tag{5}$$

where the kinetic coefficient of growth from the melt $\beta\left(T\right)$ and the undercooling at the solid-liquid interface ΔT are given respectively by

$$\beta\left(T\right) \;\simeq\; \left(\frac{a}{\lambda_0}\right)^2 a\widetilde{\nu}\frac{\Delta s}{kT}\exp\left(-\frac{\Delta s}{k}\right)\exp\left(-\frac{E}{kT}\right), \qquad (6)$$

$$\Delta T \;=\; T_m - T\ . \qquad (7)$$

3. Phase field model

The evolution of a binary dilute system to equilibrium, which consist of A-atoms (solvent) together with a tiny amount of B-atoms (solute) with the concentration C under constant temperature T and constant pressure, is described by the following set of hyperbolic equations [10, 11]:

$$\tau_D\frac{\partial^2 C}{\partial t^2} + \frac{\partial C}{\partial t} = \nabla\cdot\left[M_C\left(\frac{\partial^2 f}{\partial C^2}\nabla C + \frac{\partial^2 f}{\partial C\partial\phi}\nabla\phi\right)\right], \qquad (8)$$

$$\tau_\phi\frac{\partial^2 \phi}{\partial t^2} + \frac{\partial \phi}{\partial t} = M_\phi\left(\varepsilon_\phi^2\nabla^2\phi - \frac{\partial f}{\partial\phi}\right), \qquad (9)$$

where f is the free energy density, ϕ is the phase field variable, τ_D is the relaxation time for the diffusion flux, M_C is the mobility of B-atoms, τ_ϕ is the time scale for the relaxation of the rate of change of the phase field $\partial\phi/\partial t$, M_ϕ is the mobility of the phase field, and ε_ϕ^2 is the gradient energy factor.

According to Zhang et al. [12], the phase field dynamics at a given constant driving force ΔG with the average value, that is taken in the normal direction over the interface, is represented by

$$\Delta G = -\left\langle\Lambda^*\left(T,C,\phi\right)\right\rangle, \qquad (10)$$

with

$$\Lambda^*\left(T,C,\phi\right) = \frac{RT}{v_m}\left[\frac{\left(1-k_e\right)C}{k_e+\left(1-k_e\right)p\left(\phi\right)} - \frac{1-k_e}{m_e}\left(T-T_A\right)\right]. \qquad (11)$$

where $p\left(\phi\right) = \phi^2\left(3-2\phi\right)$ is the interpolation function, m_e is the slope of the liquidus line in the equilibrium phase diagram, T_A is the solidification temperature of the solvent, R is the gas constant, v_m is the molar volume (assumed equal for A- and B-atoms), and k_e is the equilibrium solute partition coefficient.

Under the assumption of constant averaged driving force, Eqs. (10) and (11), we have obtained from the system of governing equations (8) and (9) the following sole hyperbolic phase field equation,

$$\tau_\phi\frac{\partial^2 \phi}{\partial t^2} + \frac{\partial \phi}{\partial t} = \nu\left[\nabla^2\phi - \frac{9}{2\delta^2}\frac{dg\left(\phi\right)}{d\phi} - \frac{1}{2\sigma\delta}\Delta G\frac{dp\left(\phi\right)}{d\phi}\right]. \qquad (12)$$

where $g(\phi) = \phi^2\left(1-\phi\right)^2$ is the double-well function, ν is the phase field diffusion parameter, δ is the interfacial width, and σ is the interface energy. Note that the interface energy and the interfacial width are connected via the gradient energie factor such as $\varepsilon_\phi^2 = 2\sigma\delta$.

Using the averaging method widely known in the mechanics of continuous media [13, 14], in solidification processes [15, 16], and, particularly, in the derivation of conservation equations for multiphase systems [14, 17, 18, 19], we have evaluated the spatial and the temporal derivatives *via* interface thickness, velocity and acceleration which are driven by the average force ΔG and the interface curvature, κ [20]. These spatial and the temporal derivatives are found by choosing the phase-field profile ϕ in the dynamical regimes consistently with the traveling waves, Eq. (13), [11, 12] which are propagating in the non-stationary regime,

$$\phi(n,t) = \frac{1}{2}\left[1 + \tanh\left(\frac{n}{\ell(t)}\right)\right].\tag{13}$$

Note that the unit normal vector exterior to the solid phase $\mathbf{n}_s$ and the exterior unit normal vector to the liquid phase $\mathbf{n}_l$ are defined such as $\mathbf{n}_s = \mathbf{n}$, and $\mathbf{n}_l = -\mathbf{n}_s = -\mathbf{n}$, respectively. Also, according to Ref. [17] and references therein, the module of a phase field gradient $|\nabla\phi|$, Eq. (14), the average unit normal vector exterior to the solid phase $\mathbf{n}$, Eq. (15), and the curvature of the solid-liquid interface κ, Eq. (16), are respectively given by

$$|\nabla\phi| = \frac{\partial\phi}{\partial n}\ ,\tag{14}$$

$$\mathbf{n} = -\frac{\nabla\phi}{|\nabla\phi|}\ ,\tag{15}$$

$$\kappa = \nabla\cdot\mathbf{n} = -\frac{1}{|\nabla\phi|}\left[\nabla^2\phi - \frac{(\nabla\phi\cdot\nabla)|\nabla\phi|}{|\nabla\phi|}\right],\tag{16}$$

where the curvature takes the negative sign for the convex interfaces, $\kappa < 0$.

Therefore we have found the following spatial and temporal derivatives, Eqs. (17)-(19),

$$\nabla^2\phi = -\kappa|\nabla\phi| + \frac{(\nabla\phi\cdot\nabla)|\nabla\phi|}{|\nabla\phi|} = -\kappa\frac{\partial\phi}{\partial n} + \frac{\partial^2\phi}{\partial n^2}\ ,\tag{17}$$

$$\frac{\partial\phi}{\partial t} = -V|\nabla\phi| = -V\frac{\partial\phi}{\partial n}\ ,\tag{18}$$

$$\frac{\partial^2\phi}{\partial t^2} = -\gamma|\nabla\phi| - V\frac{\partial(|\nabla\phi|)}{\partial t} = -\gamma|\nabla\phi| + \frac{V}{\ell}\frac{\partial\ell}{\partial t}\frac{\partial\phi}{\partial n} + V^2\frac{\partial^2\phi}{\partial n^2}\ ,\tag{19}$$

where V is the velocity of the interface directed by the normal vector $\mathbf{n}$, $\gamma = \partial V/\partial t$ is the interface acceleration, and $\ell = \ell(t)$ is the time-dependent effective thickness of the interface which plays the role of the correlation length.

By incorporating the above spatial and temporal derivatives (17)-(19) in Eq. (12), we have obtained a nonlinear equation yielding the expression for the effective thickness, ℓ, Eq. (20)

$$\ell(t) = \frac{2\delta}{3}\left[1 - V^2(t)/(V_\phi)^2\right]^{1/2}\ ,\tag{20}$$

and the generalized relationship between acceleration, γ, velocity, V, curvature, κ, of the interface and the driving force, ΔG, for the interface motion as [20]:

$$\tau_\phi\frac{\gamma}{[1 - V^2/(V_\phi)^2]^{3/2}} + \frac{V}{[1 - V^2/(V_\phi)^2]^{1/2}} = \frac{\nu}{\sigma}\Delta G + \frac{\nu\kappa}{[1 - V^2/(V_\phi)^2]^{1/2}}\ .\tag{21}$$

where the maximum speed V_ϕ of the phase field propagation is defined by the relaxation time τ_ϕ, $V_\phi = (\nu/\tau_\phi)^{1/2}$.

Note that with the increase of the interface velocity, ℓ becomes smaller and, in the limit $V \to V_\phi$, the correlation length tends to zero as predicted by Eq. (20). Since the correlation length ℓ is the distance at which the essential spatial variation of the phase field occurs, one can mark that the limit $V \to V_\phi$ corresponds to a sharp change in the phase field variation. Obviously, in the steady state regime of interface propagation, i.e., in a motion with the constant normal velocity, $V \equiv const$, the correlation length (20) does not depend on time. Due to inclusion of acceleration and high interface velocity, Eq. (21) represents a general case of a

Gibbs-Thomson interfacial condition. This generalized condition can be used at the steady state regimes with constant interface velocity ($\gamma = 0$ and $V = const$) as well as at the non-stationary regimes of interface propagation ($\gamma \neq 0$ and $V \neq const$).

The limited numbers of cases and existing theories, which are connected with Eq. (21) were discussed from a theoretical point of view in [20]. Among the other important results of the dynamic boundary condition Eq. (21) for the rapidly moving curved interface which includes both velocity and acceleration of the interface and can move by mean curvature and due to the driving force given by a deviation of temperature and concentration from their equilibrium values, the following should be mentioned: (i) a generalization for the well-known velocity dependent Gibbs-Thomson relation, and (ii) a generalized Born-Infeld equation for the hyperbolic motion by mean curvature and under driving force in the traditional Cartesian coordinates. These (i) and (ii) generalizations are reduced to the classical equation for the motion by mean curvature (which follows from the Cahn-Allen equation [21, 22]) and to the standard Born-Infeld equation [23, 24] (which follows from the undamped Klein-Gordon equation).

Otherwise if the interface velocity is comparable to the maximum speed of disturbances, which have been propagating in the phase field, i.e., with $V \lesssim V_\phi$, the non-stationary propagation of the curved interface is described by the full equation (21). It is clear that the normal velocity to the interface, V, cannot overcome and be larger than the maximum speed of disturbance propagation in the phase field because the phase field itself determines the interface, its velocity and acceleration. In the case of the fast propagating planar interface, the presence of the constant velocity ($V = const$ and $\kappa = 0$), Eqs. (20) and (21) denote the velocity V as

$$V = \frac{\nu(\Delta G/\sigma)}{\sqrt{1 + (\nu/V_\phi)^2 \left(\Delta G/\sigma\right)^2}} \;, \tag{22}$$

where the driven force (Gibbs free energy difference on transformation) ΔG for a pure (chemically one component, elemental) system is given by

$$\Delta G = -\left\langle \Lambda^*\left(T, C, \phi\right)\right\rangle \equiv \frac{\Delta H}{T_m}\Delta T \;. \tag{23}$$

Table 1. Material parameters for Ni used in calculations.

Material parameter	Dimension	Value	Reference
Melting temperature, T_m	K	1706	[4]
Enthalpy of melting, ΔH	J·m^{-3}	2.66×10^9	
	J·mol^{-1}	17200	[25]
Entropy of melting, $\Delta s = \frac{\Delta H}{T_m}$	J·m^{-3}·K^{-1}	1.56×10^6	
	J·mol^{-1}·K^{-1}	10.07	[25]
Interface energy, σ	J·m^{-2}	0.25	present work
Crystal lattice parameter, a (at T_m)	m	3.565×10^{-10}	[26]
Mean distance between steps at the crystal surface, λ_0	m	$\approx 3a$	[9]
Frequency of phonon vibration, $\widetilde{\nu}$	s^{-1}	10^{14}	[9]
Activation energy, E	J·m^{-3}	2.61×10^8	
	J·mol^{-1}	1720	[25]
Diffusion coefficient for phase field, ν	m^2·s^{-1}	1.15×10^{-7}	present work
Maximum speed for phase field propagation, V_ϕ	m·s^{-1}	185	present work

4. Comparison with MD simulation in the case of nickel

Using material parameters for the nickel (see Table 1) we have tested the outcomes of the Kinetic Rate Theory and Phase Field Model in comparison with MD-data obtained in works [4, 5]. We have especially checked these approaches in a small range of undercooling (where the solid-liquid interface moves by the linear "velocity-undercooling" relationship) and for a large range of undercooling (where a clear non-linearity in the "velocity-undercooling" relationship appears in crystal growth [1]).

4.1. Small range of undercooling and overheating

Now, we compare the predictions of the equations from kinetic rate theory [9] and the nonlinear solution of the phase field model [20] with MD-data of computer simulation of Mendelev et al. [4]. These data was obtained for relatively small values of the undercooling $0 < \Delta T(\mathrm{K}) < 50$ and overheating $-55 < \Delta T(\mathrm{K}) < 0$ at the solid-liquid interface of the nickel crystal. Figure 1 shows that MD-data exhibits linear behavior for the interface velocity, both in melting and in crystallization, for the undercooling interval $-55 < \Delta T(\mathrm{K}) < 50$. It is seen clearly that Eq. (5) and Eq. (22) describe these well enough and even if we take into account the exponential equation of the kinetic rate theory, namely Eq. (4), only a very slight difference in comparison with the linearized equation; Eqs. (5) appears.
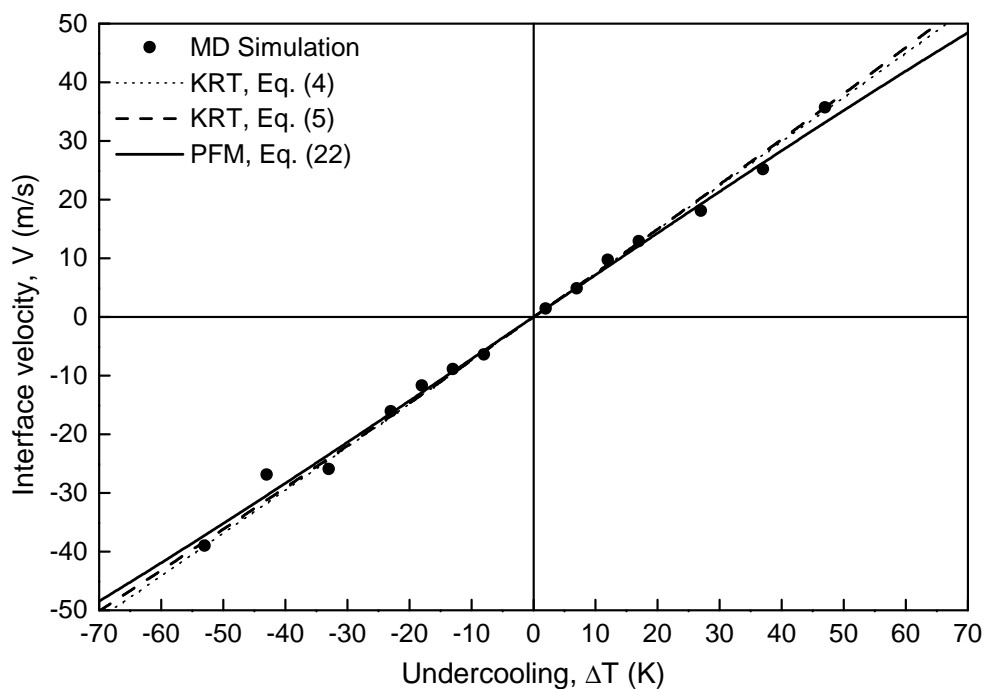

Figure 1. Comparison of the predicted interface velocity V by Eq. (4) $\cdots\cdots$ and Eq. (5) - - - - of Kinetic Rate Theory (KRT) [9], and by Eq. (22) —— of Phase Field Model (PFM) [20] with MD-data of computer simulation ● by Mendelev et al. [4] for Ni in the case of small range of undercooling $0 < \Delta T(\mathrm{K}) < 50$ and overheating $-55 < \Delta T(\mathrm{K}) < 0$.

Furthermore we have found that, for the Kinetic Rate Theory, the better correspondence to the simulated MD-data is obtained for the kinetic coefficient $\beta(T) = 0.711$ m/(s·K). This latter is a very close value, with a relative error of the order 1.1%, in comparison with the kinetic coefficient value $\beta = 0.719$ m/(s·K) given by Mendelev et al. [4], which was computed

from the results of MD-simulations. Therefore, both approaches [solutions of the phase field model Eq. (22) and linearized-and exponential equations of rate kinetics Eq. (5) and Eq. (4), respectively] confirm the ability to describe MD-data in the range of linear behavior $V \sim \Delta T$ and, relatively close to equilibrium point $\Delta T = 0$ K.

4.2. Large range of undercooling

In the present subsection, we compare the equations from kinetic rate theory [9] and the nonlinear solution of the phase field model [20] with MD-data of computer simulation obtained by Hoyt et al. [5] for large values of the undercooling $0 < \Delta T(\text{K}) < 710$ at the solid-liquid interface of nickel crystal. Figure 2 illustrates the comparison of the exponential-and linearized equations of the kinetic rate theory, Eq. (4) and Eq. (5) respectively, and of the nonlinear solution of the phase field equation, Eq. (22), with the MD-data of Hoyt et al.
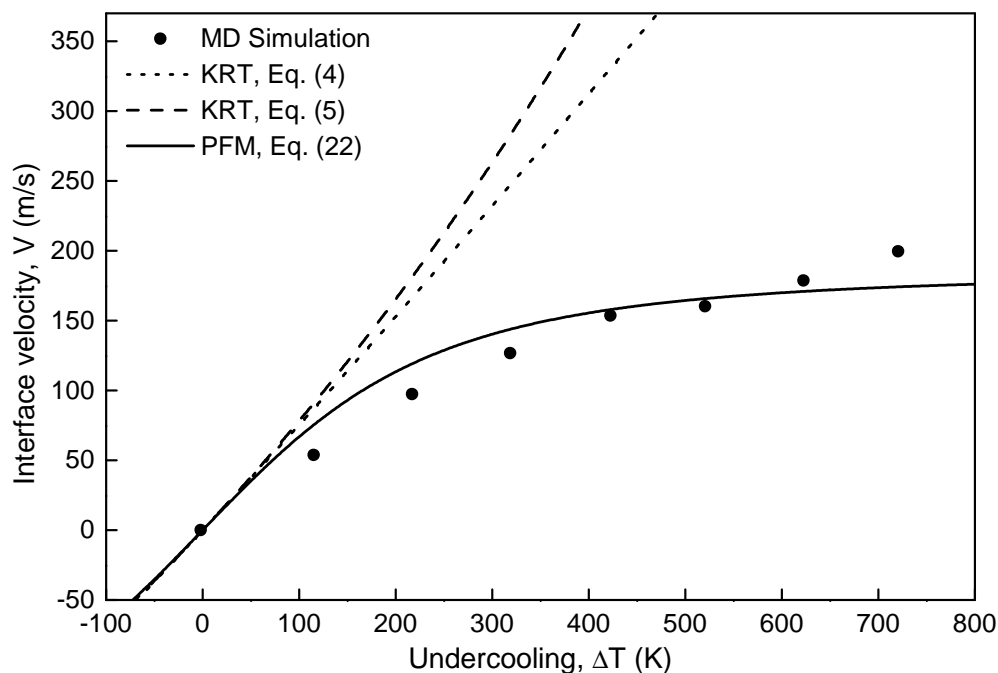

Figure 2. Comparison of the predicted interface velocity V by Eq. (4) $\cdots\cdots$ and Eq. (5) - - - - of Kinetic Rate Theory (KRT) [9], and by Eq. (22) —— of Phase Field Model (PFM) [20] with MD-data of computer simulation ● due to Hoyt et al. [5] for Ni in the case of large range of undercooling $0 < \Delta T(\text{K}) < 710$.

It can be seen that both equations of the kinetic rate theory behave inconsistently in comparison with MD-data qualitatively and, as a consequence, quantitatively. By contrast, non-linear solution of the phase field model predicts "velocity-undercooling" relationship in agreement with MD-data. Namely, the phase field equation, Eq. (22), shows that the interface velocity V gradually deviates from the linear law to smaller values as the undercooling increases. Such a behavior in crystal growth kinetics has been found by MD-simulations of elemental systems [1], qualitatively confirmed in our work [20] and presently confirmed in quantitative comparison of Eq. (22) with the MD-data of Hoyt et al. [5].

5. Conclusions

Solidification kinetics of a pure elemental substance has been analyzed. A qualitative and quantitative comparison of solid-liquid interface motion has been made. Predictions from the Kinetic Rate Theory and from the phase field model have been discussed. As a consequence of the Kinetic Rate Theory, we have considered the kinetic equation for the solid-liquid interface. From the analysis of the phase field model, we have considered the solution of Gibbs-Thomson-type equation. The kinetic equation of the Kinetic Rate Theory and the solution of Gibbs-Thomson-type equation are compared with the data of atomistic simulations obtained by method of Molecular Dynamics.

It has been shown that the Molecular-Dynamics-data of simulation for solidification or melting of a pure nickel [4] are described well by both approaches in the range of small growth velocity and within the range of relatively small undercooling (up to 50K) or small overheating (up to -55K). Within the whole (small and large) range of undercooling (up to 700K), the Kinetic Rate Theory disagrees with MD-data [5] qualitatively and quantitatively. Instead, the Gibbs-Thomson-type equation is in a good agreement with MD-data [5] within the whole range of undercooling and nickel crystal growth velocity.

6. References

[1] Hoyt J J, Asta M and Karma A 2003 Atomistic and continuum modeling of dendritic solidification *Mater. Sci. Eng.* **41** 121-64

[2] Hoyt J J, Asta M, Haxhimali T, Karma A, Napolitano R E, Trivedi R, Laird B B and Morris J R 2004 Crystal–mlt interfaces and solidification morphologies in metals and alloys *MRS Bulletin* **29** (12) 935-39

[3] Kerrache A, Horbach J and Binder K 2008 Molecular-dynamics computer simulations of crystal growth and melting in $Al_{50}Ni_{50}$ *Euro. Phys. Lett.* **81** 58001-1-6

[4] Mendelev M I, M I, Rahman M J, Hoyt J J and Asta M 2010 Molecular-dynamics study of solid–liquid interface migration in fcc metals *Model. Simul. Mater. Sci. Eng.* **18** 074002

[5] Hoyt J J, Sadigh B, Asta M and Foiles S M 1999 Kinetic phase field parameters for the Cu-Ni system derived from atomistic computations *Acta Mater.* **47** 3181–87

[6] Bragard J, Karma A, Lee Y H and Plapp M 2002 Linking phase-field and atomistic simulations to model dendritic solidification in highly undercooled melts *Inter. Sci.* **10** 121–36

[7] Berghoff M, Selzer M, and Nestler B 2013 Phase-field simulations at the atomic scale in comparison to molecular dynamics *The Scientific World Journal* **2013**, Article ID 564272 8 pages

[8] Christian J W 1975 *The Theory of Transformations in Metals and Alloys* (Oxford: Pergamon)

[9] Chernov A A 1984 *Modern Crystallography III – Crystal Growth* (Berlin: Springer)

[10] Galenko P and Jou D 2005 Diffuse-interface model for rapid phase transformations in nonequilibrium systems *Phys. Rev. E.* **71** 046125

[11] Galenko P K, Abramova E V, Jou D, Danilov D A, Lebedev V G and Herlach D M 2011 Solute trapping in rapid solidification of a binary dilute system: A phase-field study *Phys. Rev. E.* **84** 041143-1-17

[12] Zhang L, Danilova E V, Steinbach I, Medvedev D, Galenko P K 2013 Diffuse-interface modeling of solute trapping in rapid solidification: Predictions of the hyperbolic phase-field model and parabolic model with finite interface dissipation *Acta Mater.* **61** 4155–68

[13] Sou S 1971 *Hydrodynamics of Multiphase Systems* (Moscow: Mir)

[14] Drew D A 1983 Mathematical modeling of two-phase flow *Ann. Rev. Fluid Mech.* **15** 261–91

[15] Zhuravlev V A and Kitaev E M 1974 *Thermophysics of Continuous Ingot Formation* (Moscow: Metallurgia)

[16] Vorobiov I L 1980 *Proceedings of Bauman-MVTU* **30** 31

[17] Beckermann C, Diepers H J, Steinbach I, Karma A and Tong X 1999 Modeling melt convection in phase-field simulations of solidification *J. Comput. Phys.* **154** 468–96

[18] Hassanizadeh M. and Gray W.G. 1979 General conservation equations for multi-phase systems: 1. Averaging procedure *Adv. Water Resour.* **2** 131–44

[19] Ni J and Beckermann C A 1991 Volume-averaged two-phase model for transport phenomena during solidification *Metall. Trans.* B. **22** 349–61

[20] Salhoumi A and Galenko P K 2016 Gibbs-Thomson condition for the rapidly moving interface in a binary system *Physica* A **447** 161–71

[21] Cahn J W and Allen S M 1977 microscopic theory of domain wall motion and its experimental verification in Fe-Al alloy domain growth kinetics *J. Phys. Colloq.* **38** C7–51–54

[22] Allen S M and Cahn J W 1979 A microscopic theory for antiphase boundary motion and its application to antiphase domain coarsening *Acta Metall.* **27** 1085–95

[23] Born M and Infeld L 1934 Foundations of the new field theory *Proc. R. Soc. A Math. Phys. Eng. Sci.* **144** 425–51

[24] Whitham G B 1974 *Linear and Nonlinear Waves* (New York: Wiley-Interscience)

[25] Galenko P K and Danilov D A 2000 Hyperbolic self-consistent problem of heat transfer in rapid solidification of supercooled liquid *Phys. Lett.* A. **278** 129–38

[26] Davey W P 1925 Precision measurements of the lattice constants of twelve common metals *Phys. Rev.* **25** 753–61

Acknowledgments